



# Catalytic and Photocatalytic Nitrate Reduction Over Pd-Cu Loaded Over Hybrid Materials of Multi-Walled Carbon Nanotubes and TiO<sub>2</sub>

Cláudia G. Silva\*, Manuel F. R. Pereira, José J. M. Órfão, Joaquim L. Faria and Olívia S. G. P. Soares

Laboratory of Separation and Reaction Engineering-Laboratory of Catalysis and Materials (LSRE-LCM), Faculdade de Engenharia, Universidade do Porto, Porto, Portugal

## OPEN ACCESS

### Edited by:

Zhimin Ao,  
Guangdong University of Technology,  
China

### Reviewed by:

Priyabrat Mohapatra,  
C. V. Raman College of Engineering,  
India  
Miguel Angel Centeno,  
Instituto de Ciencia de Materiales de  
Sevilla (ICMS), Spain

### \*Correspondence:

Cláudia G. Silva  
cgsilva@fe.up.pt

### Specialty section:

This article was submitted to  
Green and Sustainable Chemistry,  
a section of the journal  
Frontiers in Chemistry

Received: 01 August 2018

Accepted: 05 December 2018

Published: 20 December 2018

### Citation:

Silva CG, Pereira MFR, Órfão JJM,  
Faria JL and Soares OSGP (2018)  
Catalytic and Photocatalytic Nitrate  
Reduction Over Pd-Cu Loaded Over  
Hybrid Materials of Multi-Walled  
Carbon Nanotubes and TiO<sub>2</sub>.  
Front. Chem. 6:632.  
doi: 10.3389/fchem.2018.00632

TiO<sub>2</sub> and carbon nanotube-TiO<sub>2</sub> hybrid materials synthesized by sol-gel and loaded with 1%Pd–1%Cu (%wt.) were tested in the catalytic and photocatalytic reduction of nitrate in water in the presence of CO<sub>2</sub> (buffer) and H<sub>2</sub> (reducing agent). Characterization of the catalysts was performed by UV-Vis and fluorescence spectroscopy, X-ray diffraction, temperature programmed reduction, N<sub>2</sub> adsorption, and electron microscopy. The presence of light produced a positive effect in the kinetics of nitrate removal. Higher selectivity toward nitrogen formation was observed under dark condition, while the photo-activated reactions showed higher selectivity for the production of ammonium. The hybrid catalyst containing 20 %wt. of carbon nanotubes shows the best compromise between activity and selectivity. A mechanism for the photocatalytic abatement of nitrate in water in the presence of the hybrid materials was proposed, based in the action of carbon nanotubes as light harvesters, dispersing media for TiO<sub>2</sub> particles and as charge carrier facilitators.

**Keywords:** photocatalysis, catalytic reduction, nitrate, titanium dioxide, carbon nanotubes, palladium, copper

## INTRODUCTION

Nitrate is a naturally occurring ion that is part of the nitrogen cycle, in which nitrogen species are switched between organisms and the environment. The increasing use of inorganic nitrogenous fertilizers, the disposal of wastes (mainly from oxidation of nitrogenous waste products in human and animal excreta) and changes in land use are the main causes accounting for the progressively increasing levels of this pollutant in groundwater supplies. Nitrate ion (NO<sub>3</sub><sup>-</sup>) is the stable form of combined nitrogen for oxygenated systems and is potentially hazardous for humans, since it can be transformed into nitrite in the human body, which may cause the blue baby syndrome, being also a precursor of carcinogenic nitrosamines (Kapoor and Viraraghavan, 1997). Moreover, it may cause the eutrophication of rivers and lakes. The maximum contaminant level in drinking water of nitrogen species as nitrate, nitrite, and ammonium is 50, 0.5, and 0.5 mg/L, respectively (EU Water Framework Directive<sup>1</sup>).

<sup>1</sup>EU Water Framework Directive (2000). Available online at: [http://ec.europa.eu/environment/water/water-framework/index\\_en.html](http://ec.europa.eu/environment/water/water-framework/index_en.html) (Accessed 2018).

The removal of nitrate from water constitutes a great challenge to safeguarding drinking water resources of suitable quality. In this context, a great effort has been put in the development of water technologies capable to address the environmental and health concerns. Conventional methods are based in physical-chemical treatment processes (reverse osmosis, ion exchange, and electro dialysis) and biological denitrification.

Heterogeneous catalytic systems like catalytic and photocatalytic reduction of nitrate have been shown to be promising processes compared to conventional treatments (Sá et al., 2009; Soares et al., 2011a, 2014; Luiz et al., 2012; Shand and Anderson, 2013). Catalytic nitrate reduction occurs by consecutive and parallel reactions where nitrate is reduced to nitrite, which is converted to ammonium, as undesired by-product, and to nitrogen, as desired product. The main issue of this process is the selectivity toward nitrogen, which is often compromised. Bimetallic catalysts composed by a noble metal (Pd, Pt, or Rh) and a promoter metal (Cu, Sn, or In) supported on different materials are the most used for catalytic hydrogenation of nitrate (Soares et al., 2009; Calvo et al., 2010; Marchesini et al., 2010; Wada et al., 2012), although monometallic catalysts also present some activity depending on the support (Barrabés et al., 2010; Anderson, 2011; Devadas et al., 2011). Pd-Cu catalysts are normally the most efficient, Pd-Sn and Pd-In also presenting good performances (Martínez et al., 2017). In the case of photocatalytic reduction, besides the type of metal catalysts, several other conditions such as the catalyst support, the pH of the solution, the irradiation source, nature of the reducing agent or electron donor (hole scavenger) also affect the performance of the process. H<sub>2</sub> and CO<sub>2</sub> are usually used in catalytic reduction reactions, in which H<sub>2</sub> serves as reductant and CO<sub>2</sub> as buffer (Prusse et al., 2000). In the case of the photo-assisted catalytic process, oxalic acid, formic acid, or methanol are the most used hole scavengers (Zhang et al., 2005; Doudrick et al., 2013).

Titanium dioxide-based materials are the most widely used catalysts for the photocatalytic reduction of nitrate, the bimetallic Pd-Cu/TiO<sub>2</sub> and Pt-Cu/TiO<sub>2</sub> being the ones showing most promising results. On the other hand, Pd-Cu catalysts supported on carbon materials and also in metal oxides are the most used for nitrate catalytic reduction. TiO<sub>2</sub>-based catalysts are normally highly active for nitrate removal, yet, due to their capacity to drive hydrogenation, low nitrogen selectivity is reached (Sá et al., 2005). It has been reported that the activity of Pd-Cu bimetallic catalysts supported on carbon materials was higher than the same Pd-Cu catalyst supported on a metal oxide, such as TiO<sub>2</sub>, Al<sub>2</sub>O<sub>3</sub>, SiO<sub>2</sub>, or ZrO<sub>2</sub>, at the same operating conditions, due to their surface chemistry and higher metals dispersion (Sakamoto et al., 2006; Soares et al., 2011a). Moreover, the coupling of carbon nanotubes with TiO<sub>2</sub> has proved to induce a positive effect in the activity and selectivity of Pd-Cu catalysts for the catalytic reduction of nitrate into N<sub>2</sub> (Soares et al., 2011a).

Following the previous findings, in the present work we explored the synergies between carbon nanotubes (CNT) and titanium dioxide in both catalytic and photocatalytic reduction of nitrate in water. For that purpose, hybrid materials of TiO<sub>2</sub> with different CNT contents, and loaded with 1%Pd and 1%Cu (wt.%) were evaluated as catalysts. Hydrogen and carbon dioxide were used as reducing and pH buffer agents, respectively. The

materials were tested under the same experimental conditions, the only difference between the two processes being the introduction of a near-UV to visible light source in the case of the photocatalytic reactions.

## EXPERIMENTAL

### Catalysts Preparation

Multi-walled carbon nanotubes synthesized by catalytic decomposition of CH<sub>4</sub> were purchased from Shenzhen Nanoport Co. Ltd (purity > 95%, diameter < 10 nm; length = 5–15 μm). TiO<sub>2</sub> and CNT-TiO<sub>2</sub> composite catalysts were prepared through an acid-catalyzed sol-gel procedure, as described elsewhere (Silva and Faria, 2010). Briefly, TiO<sub>2</sub> was prepared by dissolving Ti(OC<sub>3</sub>H<sub>7</sub>)<sub>4</sub> (Aldrich 97%) in ethanol. The solution was magnetically stirred for 30 min, and then nitric acid (Fluka 65%) was added.

For the composite catalysts preparation, a certain amount of CNT was added to the Ti(OC<sub>3</sub>H<sub>7</sub>)<sub>4</sub> ethanol solution. The mixture was kept stirring until a homogenous gel was formed. The gel was left aging in air for 5 days. The resulting material was then crushed into a fine powder (particle size < 100 μm). The powders were calcined at 400°C under a flow of N<sub>2</sub> for 2 h to obtain TiO<sub>2</sub> or CNT-TiO<sub>2</sub> hybrid materials. Catalysts were labeled as XCNT-TiO<sub>2</sub>, where X (5, 10, 20, 50, 70, and 90) corresponds to the weight percentage of CNT in the material.

The monometallic (Pd) and bimetallic (Pd-Cu) catalysts were prepared by incipient wetness impregnation and co-impregnation, respectively. Briefly, aqueous solutions containing the proper mass of the corresponding salts [PdCl<sub>2</sub>, Alfa Aesar 99.9%; Cu(NO<sub>3</sub>)<sub>2</sub>, Riedel-de Haen 99%] were added dropwise to TiO<sub>2</sub> and CNT-TiO<sub>2</sub> materials. In the case of the bimetallic catalyst, the materials were co-impregnated with a solution containing both precursor salts. The palladium and copper contents were fixed at 1%Pd-1%Cu and 1%Pd (weight percentages). After impregnation, the metal-loaded materials were dried in an oven at 100°C for 24 h. Then, the catalysts were heat treated under a nitrogen flow at 200°C for 1 h. At the end of this period, the gas stream was switched to hydrogen for 3 h to promote metals reduction. Finally, the materials were left to cool down to room temperature under a nitrogen flow.

### Catalysts Characterization

Powder X-ray Diffraction (XRD) analysis was performed on a Philips X'PertMPD diffractometer (Cu-Kα = 0.15406 nm). The Brunauer-Emmett-Teller (BET) specific surface area (S<sub>BET</sub>) was determined from N<sub>2</sub> adsorption-desorption isotherms at 196°C, in a Quantachrome Nova 4200e apparatus. Temperature programmed reduction (TPR) was carried out in an AMI-200 (Altamira Instruments) system. The H<sub>2</sub> consumption was followed by a thermal conductivity detector (TCD) and by a mass spectrometer (Dymaxion 200 amu, Ametek). Transmission electron microscopy (TEM) micrographs were obtained using a LEO 906E microscope operating with an accelerating voltage of 120 kV. Diffuse reflectance (DR) UV-Vis spectra of the powder samples were recorded on a JASCO V-560 UV-Vis spectrophotometer, equipped with an integrating sphere attachment (JASCO ISV-469). The

reflectance spectra were converted by the instrument software (JASCO) to equivalent absorption Kubelka–Munk units. Steady-state photoluminescence (PL) spectra were recorded at room temperature on a JASCO FP-8300 spectrofluorometer equipped with a 150 W Xe lamp. The morphology and elemental mapping of the materials was obtained by SEM/EDXS analysis using a FEI Quanta 400FEG ESEM/EDAX Genesis X4M instrument.

## Catalytic and Photocatalytic Nitrate Reduction Experiments

The catalytic and photocatalytic experiments were carried out in a glass cylindrical reactor. Initially, 190 mL of deionised water and 100 mg of catalyst were fed into the reactor. When used, a gas mixture of H<sub>2</sub> and CO<sub>2</sub> [1:1 flow rate = 200 cm<sup>3</sup> (STP) min<sup>-1</sup>] was passed through the reactor to remove the dissolved oxygen; CO<sub>2</sub> acts as pH buffer (pH = 5.5). A Heraeus TQ 150 medium pressure mercury vapor lamp ( $\lambda_{\text{exc}} = 254, 313, 365, 436, \text{ and } 546 \text{ nm}$ ) was used as radiation source. The lamp was located axially in the reactor and held in a quartz immersion tube. A DURAN<sup>®</sup> glass jacket was used as water circulating cooling system (temperature maintained at 25°C) and as a filter for cutting-off low wavelength UV lines and letting pass radiation in the near-UV to visible light range ( $\lambda_{\text{exc}} \geq 365 \text{ nm}$ ). Before turning illumination on, the solution was magnetically stirred in the dark for 15 min. After that period, 10 mL of a nitrate solution, prepared from NaNO<sub>3</sub> (Sigma-Aldrich 99%), was added to the reactor, in order to obtain an initial NO<sub>3</sub><sup>-</sup> concentration of 100 mg L<sup>-1</sup>. The first sample was taken out just before the light was turned on, in order to determine the initial nitrate concentration in solution. The catalytic (dark) experiments were carried out under the same experimental conditions, but in the absence of light.

Samples were withdrawn regularly from the reactor, and centrifuged before determination of NO<sub>3</sub><sup>-</sup>, NO<sub>2</sub><sup>-</sup>, and NH<sub>4</sub><sup>+</sup> concentrations. NO<sub>3</sub><sup>-</sup> and NO<sub>2</sub><sup>-</sup> were simultaneously determined by HPLC using a Hitachi Elite Lachrom system equipped with a diode array detector. The stationary phase was a Hamilton PRP-X100 column (150 × 4.1 mm) working at room temperature, under isocratic conditions. The mobile phase was a solution of 0.1 M NaCl:CH<sub>3</sub>OH (45:55). The concentration of NH<sub>4</sub><sup>+</sup> was determined by potentiometry.

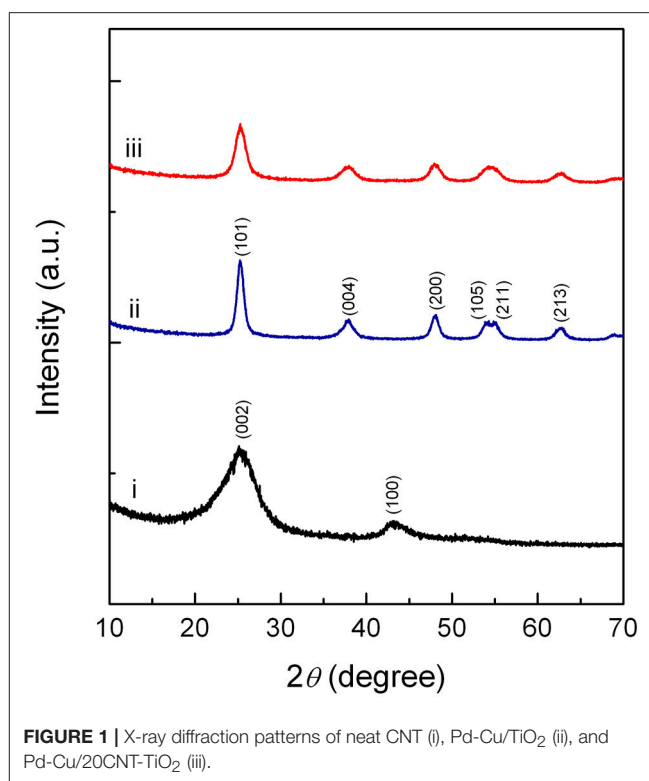
Palladium and copper leaching was assessed after each experiment by atomic absorption spectrometry (UNICAM 939/959), the absence of metals (within the experimental error) being confirmed for all the cases.

Reproducibility tests were performed for selected experiments, the results being in agreement with a maximum error of about 2.5%. NO<sub>3</sub><sup>-</sup> conversion and the selectivity to NO<sub>2</sub><sup>-</sup> and NH<sub>4</sub><sup>+</sup> were calculated as described elsewhere (Soares et al., 2014).

## RESULTS AND DISCUSSION

### Catalysts Characterization

XRD patterns of neat CNT, Pd-Cu/TiO<sub>2</sub>, and Pd-Cu/20CNT-TiO<sub>2</sub> are displayed in **Figure 1**. Typical (002) and (100) diffraction lines are evident in the XRD pattern of CNT. XRD



analysis of TiO<sub>2</sub> and CNT-TiO<sub>2</sub> composites revealed that only anatase phase is present in neat TiO<sub>2</sub> and composite catalysts. The XRD patterns of the Pd-Cu loaded CNT-TiO<sub>2</sub> materials are very similar to the one of Pd-Cu/TiO<sub>2</sub>, with the CNT contribution hardly been identified. The Cu and Pd phases were not detected by XRD, which must be related to the low metal percentages (1%wt.). Anatase crystallites of 8.5 nm average size were found for neat TiO<sub>2</sub>, as determined by the Scherrer equation and confirmed by TEM (**Figure 2a**). The sizes of the anatase crystallites present at the composite catalysts decreased with increasing carbon content, suggesting that CNT may act as dispersing medium for TiO<sub>2</sub> particle precursors during the crystallization process (**Table 1**).

The BET surface areas ( $S_{\text{BET}}$ ) of TiO<sub>2</sub> and CNT-TiO<sub>2</sub> materials are listed in **Table 1**. Materials with lower carbon content, namely 5CNT-TiO<sub>2</sub> and 10CNT-TiO<sub>2</sub> composites, showed surface areas lower than the ones estimated through the mass composition of the composites ( $S_{\text{BET,calc}}$ ) and even lower than for neat TiO<sub>2</sub>. These results indicate that the presence of low amounts of CNT induces the formation of big TiO<sub>2</sub> crystallite agglomerates, therefore decreasing the surface area of the composite catalyst (**Figure 2b**).

With the carbon content increasing up to 20% (20CNT-TiO<sub>2</sub>), the presence of a larger amount of CNT seems to prevent TiO<sub>2</sub> particles from agglomerating, thus increasing the surface area, which was even higher than the calculated ( $S_{\text{BET,calc}}$ ). This was confirmed by TEM (**Figure 2c**), where TiO<sub>2</sub> particles of very small dimensions can be observed surrounding the sidewalls of CNT. In the case of the composite with

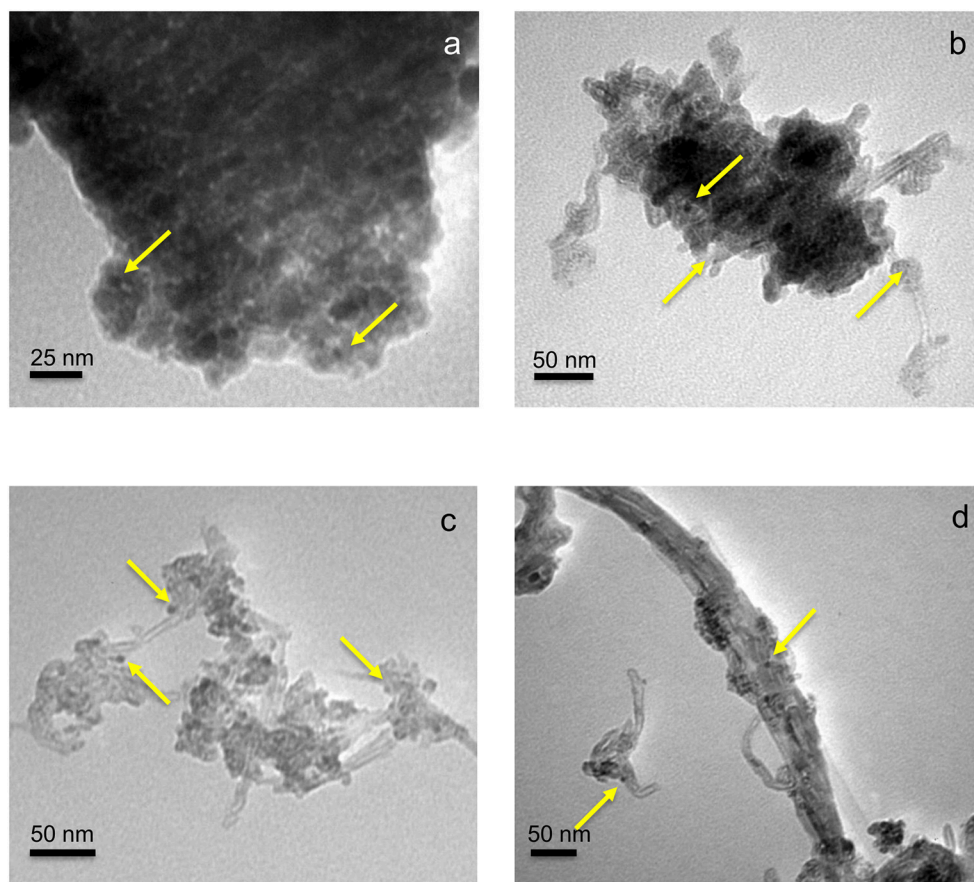


**FIGURE 2** | TEM micrographs of TiO<sub>2</sub> (a), 5CNT-TiO<sub>2</sub> (b), 20CNT-TiO<sub>2</sub> (c), and 70CNT-TiO<sub>2</sub> (d) loaded with 1% Cu and 1% Pd (wt. %). The arrows indicate the presence of metal nanoparticles.

similar amounts of TiO<sub>2</sub> and CNT phases (50CNT-TiO<sub>2</sub>), the values for  $S_{\text{BET}}$  and  $S_{\text{BET,calc}}$  were similar. Nevertheless, a further increase on the amount of CNT revealed to have a detrimental effect on the surface area of the resulting composites. A decrease in the  $S_{\text{BET}}$  in relation to the calculated values of 15 and 40% was observed for 70CNT-TiO<sub>2</sub> and 90CNT-TiO<sub>2</sub> materials, respectively, which may be attributed to the formation of CNT bundles decreasing the accessible surface area, as could be visualized by TEM for 70CNT-TiO<sub>2</sub> (Figure 2d). Due to the low amount of metals used, the textural properties of the metal-loaded catalysts remained practically unchanged compared to the pristine supports. The presence of metal particles of very small dimensions (lower than 10 nm) loaded on the TiO<sub>2</sub>-based materials could be observed by TEM (Figure 2).

SEM-EDXS analysis of Pd-Cu/TiO<sub>2</sub> (Figure 3a) and Pd-Cu/20CNT-TiO<sub>2</sub> (Figure 3b) revealed that Pd and Cu nanoparticles are well dispersed in the catalysts, with no apparent prevalence of one of the metals.

The carbon content of the CNT-TiO<sub>2</sub> composites determined by TG analysis ( $C_{\text{TG}}$ ) agrees fairly well with the nominal percentage, indicating negligible gasification of CNT during the calcination step (Table 1).

**TABLE 1** | Surface area, carbon content, and dimensions of the anatase crystallites of TiO<sub>2</sub> and CNT-TiO<sub>2</sub> composites.

Catalyst	$S_{\text{BET}}$ (m <sup>2</sup> g <sup>-1</sup> )	$S_{\text{BET,calc}}$ (m <sup>2</sup> g <sup>-1</sup> )	$C_{\text{TG}}$ (%)	$d_{\text{A}}$ (nm)
TiO <sub>2</sub> -SG	107	–	–	8.5
CNT	185	–	–	–
5CNT-TiO <sub>2</sub>	70	110	3.5	11.2
10CNT-TiO <sub>2</sub>	94	113	7.6	9.4
20CNT-TiO <sub>2</sub>	131	120	17	8.3
50CNT-TiO <sub>2</sub>	147	143	46	7.2
70CNT-TiO <sub>2</sub>	111	130	71	6.5 <sup>a</sup>
90CNT-TiO <sub>2</sub>	104	174	86	<i>n.d.</i>

<sup>a</sup>Determined by TEM; *n.d.*, not determined.

Figure 4 shows the TPR profiles for both TiO<sub>2</sub> and 20CNT-TiO<sub>2</sub> materials, which were obtained before heat-treating the metal salt-loaded supports. Both materials show a reduction peak centered at 150°C, assigned to the reduction of Cu oxides promoted by the presence of Pd (Soares et al., 2011a). The thermal treatment under

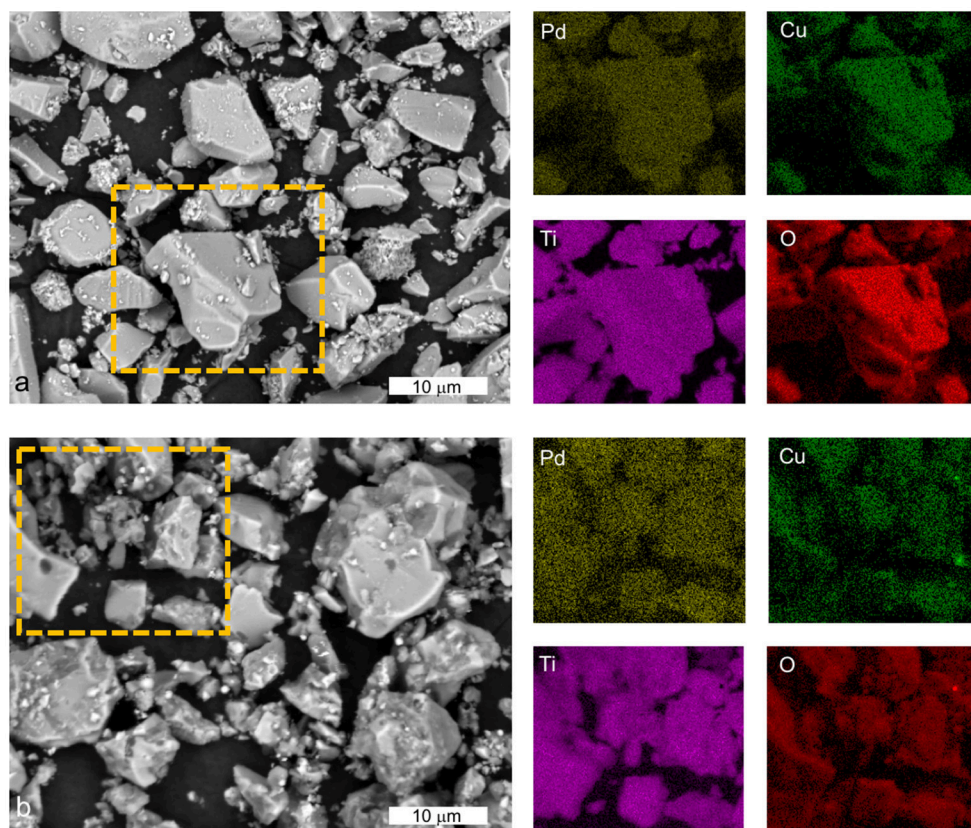


**FIGURE 3** | SEM-EDX analysis of Pd-Cu/TiO<sub>2</sub> (a) and Pd-Cu/20CNT-TiO<sub>2</sub> (b) with the respective elemental mapping for Pd, Cu, Ti, and O in the selected regions (dashed rectangle).

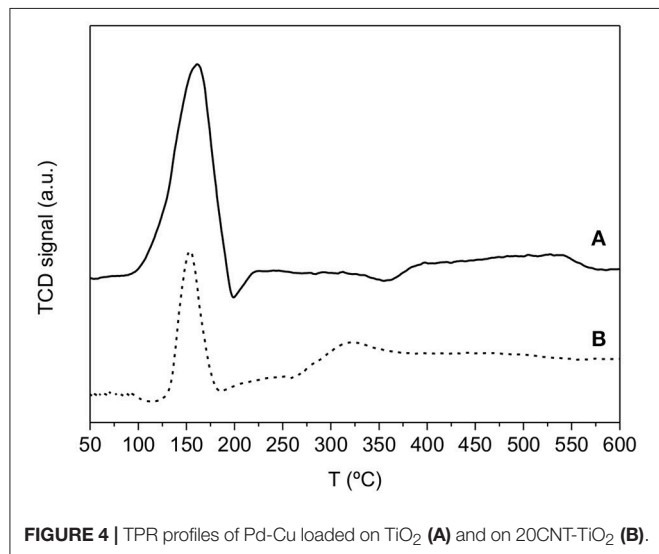


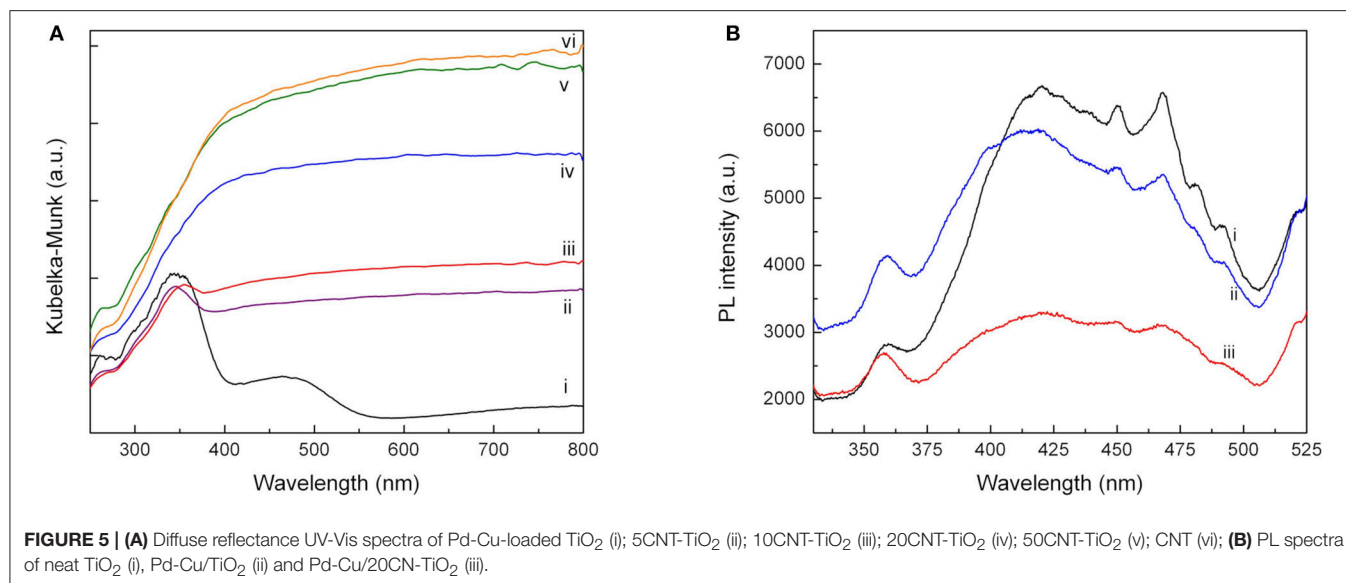
**FIGURE 4** | TPR profiles of Pd-Cu loaded on TiO<sub>2</sub> (A) and on 20CNT-TiO<sub>2</sub> (B).

H<sub>2</sub> should produce Pd and Cu particles in the reduced form, i.e., Pd<sup>0</sup> and Cu<sup>0</sup> (Soares et al., 2010, 2011a). Similar results were obtained for the remaining CNT-TiO<sub>2</sub> composite materials.

DR UV-Vis analysis of Pd-Cu/TiO<sub>2</sub> (Figure 5A) shows the TiO<sub>2</sub> characteristic absorption band at wavelength below 400 nm, a band peaking at c.a. 480 nm attributed to the presence of Pd and a broad absorption band rising from 550 nm due to the occurrence of Cu species (López et al., 2009; Wu et al., 2009; Soares et al., 2014).

As expected, the presence of CNT led to a rise of light absorption in the visible spectral region, increasing with the CNT content on the composite catalysts up to a CNT load of 50 wt.%. This behavior has been attributed not only to the capacity of CNT to absorb visible light but also to an increment of surface electronic species availability and mobility in the composite catalysts due to the introduction of CNT, as already reported in previous studies (Silva and Faria, 2010; Dai et al., 2014). A further increase in the CNT content did not produce any effect on the optical absorption of the composite materials. Moreover, the absorption peaks of the metal species could not be identified in the UV-Vis spectra of the composite materials, which may be attributed to a higher dispersion of the metal particles when supported on the composite materials.

The photoluminescence (PL) spectra were performed for having an insight in the behavior of light-generated electronic species in photocatalysts, since PL emission results from the recombination of electrons and holes. The PL emission spectra



of the pure neat TiO<sub>2</sub> and Pd-Cu loaded TiO<sub>2</sub> and 20CNT-TiO<sub>2</sub> materials excited at 280 nm are shown in **Figure 5B**. The PL signal observed for neat TiO<sub>2</sub> can be attributed to the transition of electrons from the oxygen vacancies to TiO<sub>2</sub> valence band (Tahir et al., 2017). After loading TiO<sub>2</sub> with Pd and Cu, an increase in the PL intensity was observed in the range from 330 to 400 nm, which may be attributed to the higher availability of photoexcited electrons in the bimetallic catalyst. Yet, a decrease in the PL signal intensity in the 400–525 nm range is observed, meaning that electron-hole recombination was decreased by the presence of the metal nanoparticles. Pd-Cu/20CNT-TiO<sub>2</sub> shows a very significant decrease in the PL intensity as compared with bare and metal loaded TiO<sub>2</sub>, indicating highly efficient inhibition of charge carriers recombination and suggesting the existence of electronic synergies between the metals and the hybrid CNT-TiO<sub>2</sub> material (Zhang et al., 2012).

## Catalytic and Photocatalytic Nitrate Reduction

TiO<sub>2</sub> and CNT-TiO<sub>2</sub> composites loaded with 1%Pd and 1%Cu (wt.%) were used for catalytic and photocatalytic reduction of nitrate in aqueous suspensions. Monometallic Pd-TiO<sub>2</sub> was used for comparison purposes. H<sub>2</sub> and CO<sub>2</sub> were continuously added to the reaction media, acting as reducing agent and pH buffer, respectively. The materials were tested under the same experimental conditions, the only difference between the two processes being the introduction of a near-UV to visible light source in the case of the photocatalytic reactions.

The performances of the different catalysts for the (dark) catalytic reduction process are presented in **Figure 6A**. Very low nitrate conversion (4%) was achieved using the monometallic Pd-TiO<sub>2</sub> catalyst, the presence of Cu being fundamental for the reaction to occur. Moreover, as expected, it can be observed that the support has a crucial influence on the performance of the bimetallic catalysts.

In the case of the catalytic reduction process, Pd-Cu/TiO<sub>2</sub> was the most efficient catalyst in terms of the kinetics of nitrate removal, with total nitrate conversion being achieved at the end of 90 min of reaction. Similar kinetic behavior was observed for nitrate reduction reactions using the composite materials with a CNT load (Y) of 5, 10, and 20%, leading to total nitrate removal at the end of 120 min of reaction. For higher CNT loads, a progressive detrimental effect in the kinetics of nitrate removal has been observed. Nitrate conversions of 95, 79, and 27% have been obtained at the end of 240 min when using composites with Y = 50, 70, and 90%, respectively. For the Pd-Cu/CNT catalyst only 12% nitrate removal was achieved at the end of the catalytic run.

In general, the presence of light promotes a positive effect in nitrate removal (**Figure 6B**). As in the case of the (dark) catalytic process, the simultaneous presence of Pd and Cu was a *sine qua non* condition for nitrate conversion to occur. The composite material with the lowest CNT content (Y = 5%) produced a decrease in the efficiency of nitrate abatement compared to Pd-Cu/TiO<sub>2</sub>. Yet, a further increase in the CNT load up to Y = 20% lead to a rise in the rate of nitrate removal. For the composites with higher CNT content (Y = 50, 70, and 90%) a progressive loss in the efficiency toward NO<sub>3</sub><sup>-</sup> conversion was observed.

The conversion of nitrate at 60 min of reaction was calculated in order to get a better understanding of the effect of CNT load in the kinetics of NO<sub>3</sub><sup>-</sup> removal by both catalytic and photocatalytic routes (**Figure 6C**). It is notorious that the amount of CNT plays a role in the efficiency of the composite materials. As already mentioned, composite materials underperformed TiO<sub>2</sub> in catalytic nitrate reduction with a decrease in the nitrate conversion with increasing CNT load. Yet, for the photocatalytic process a positive effect was observed using 10CNT-TiO<sub>2</sub> and, in particular, 20CNT-TiO<sub>2</sub> comparing with the experiments using TiO<sub>2</sub> as support. On the other hand, the bimetallic catalyst supported on 20CNT-TiO<sub>2</sub> promotes total conversion of nitrate at 60 min of reaction. Reutilization tests were performed

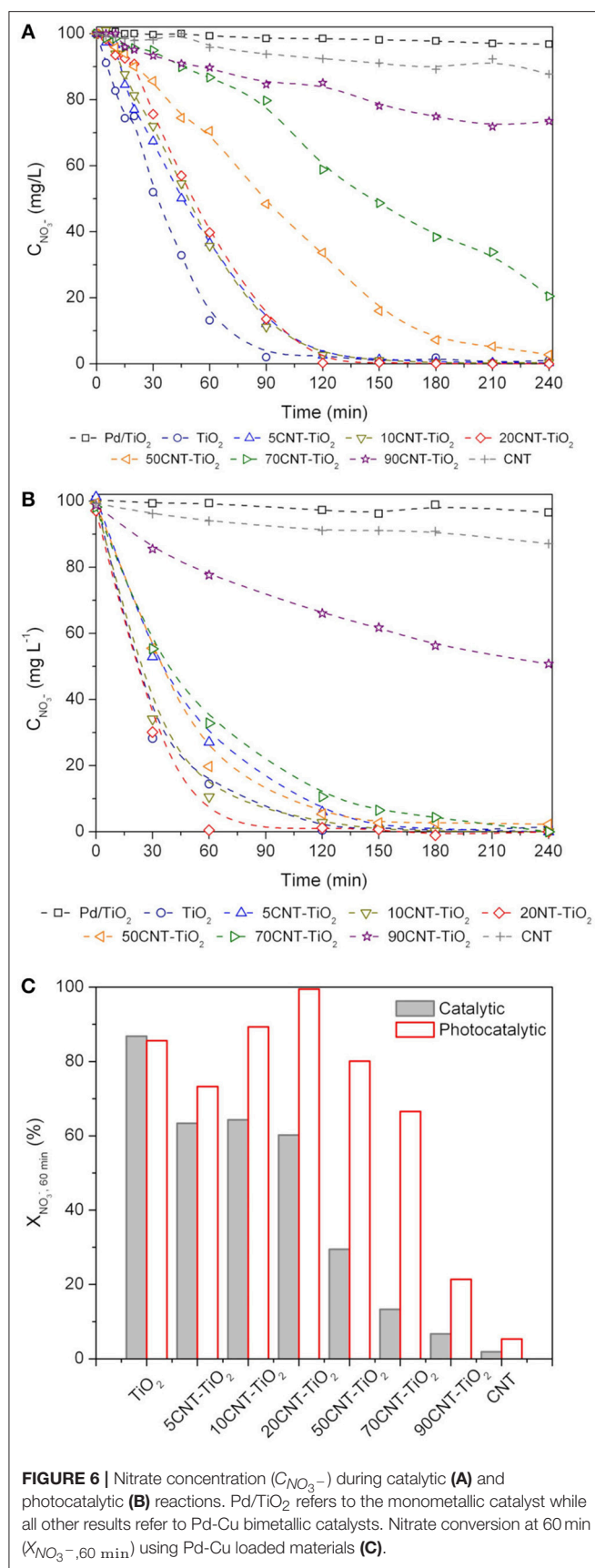


**FIGURE 6** | Nitrate concentration ( $C_{NO_3^-}$ ) during catalytic (A) and photocatalytic (B) reactions. Pd/TiO<sub>2</sub> refers to the monometallic catalyst while all other results refer to Pd-Cu bimetallic catalysts. Nitrate conversion at 60 min ( $X_{NO_3^-,60\text{ min}}$ ) using Pd-Cu loaded materials (C).

using Pd-Cu/20CNT-TiO<sub>2</sub> and Pd-Cu/TiO<sub>2</sub> under catalytic and photocatalytic conditions. In both cases the results indicate that the performance of the catalysts was maintained within 5% variation over 3 consecutive runs.

**Figure 7** shows the nitrite and ammonium profiles during catalytic and photocatalytic reactions using Pd-Cu loaded TiO<sub>2</sub>, CNT, and 20CNT-TiO<sub>2</sub> catalysts. Residual amounts of NO<sub>2</sub><sup>-</sup> and NH<sub>4</sub><sup>+</sup> were produced using Pd-Cu/CNT during both catalytic and photocatalytic processes. When Pd-Cu/TiO<sub>2</sub> was used as catalyst, nitrite is partially transformed into ammonia during the reaction, which is accumulated in the aqueous media. It was found that for the catalytic process, the formation of nitrite and conversion into ammonium is slower than for the photocatalytic process. Also, lower amounts of ammonia were produced in the presence of light, using Pd-Cu/TiO<sub>2</sub> and Pd-Cu/CNT, meaning a higher selectivity of the photocatalytic process toward N<sub>2</sub> formation.

For the reactions using Pd-Cu/20CNT-TiO<sub>2</sub> higher amounts of NO<sub>2</sub><sup>-</sup> were found during the catalytic and photocatalytic reactions, which were completely depleted at the end of 180 and 60 min of reaction, respectively (**Figure 7A**). Yet, contrarious to what was observed for the reactions using Pd-Cu/TiO<sub>2</sub> and Pd-Cu/CNT, the use of the metal-loaded 20CNT-TiO<sub>2</sub> catalyst under irradiation lead to the formation of higher amounts of ammonia when compared to the catalytic process (**Figure 7B**).

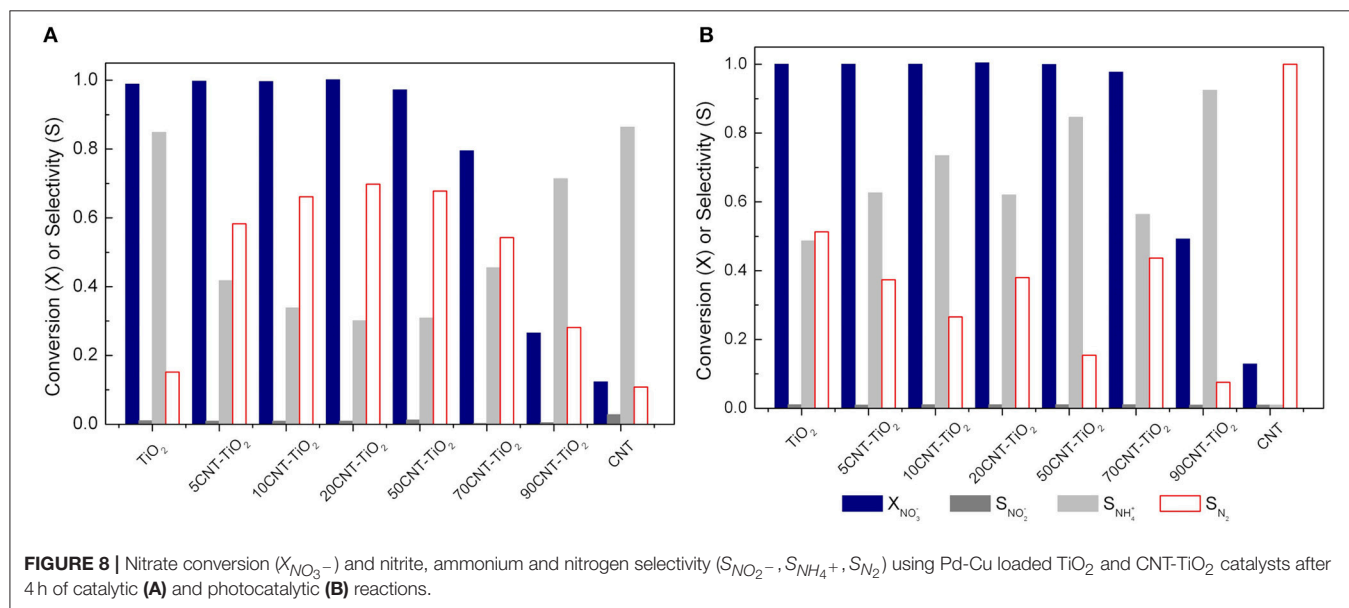
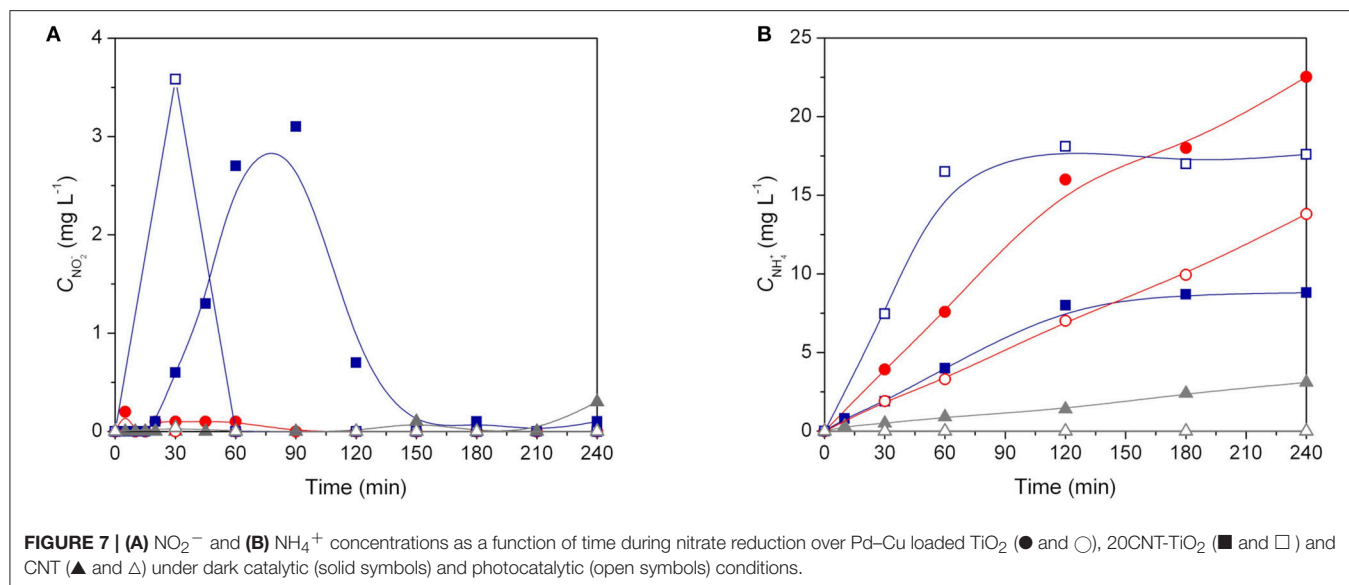
## Catalytic and Photocatalytic Nitrate Reduction Mechanisms Using CNT-TiO<sub>2</sub> Catalysts

As described above, nitrate reduction over CNT-TiO<sub>2</sub> hybrid materials behave very differently in dark conditions and under irradiation. Although the photo-assisted process provide a quicker depletion of NO<sub>3</sub><sup>-</sup>, the selectivity toward N<sub>2</sub> is greatly affected by the use of CNT-TiO<sub>2</sub> hybrid materials as Pd-Cu supports (**Figure 8**).

In the case of the catalytic reduction process, an increase in N<sub>2</sub> selectivity is observed with increasing CNT content up to 20 wt.%. A further increase in the amount of CNT led to a progressive decrease in the selectivity toward N<sub>2</sub> formation (**Figure 8A**). On the other hand, the photocatalytic reduction of NO<sub>3</sub><sup>-</sup> using CNT-TiO<sub>2</sub> catalysts appeared to be more selective for the reduction of nitrate into ammonia (**Figure 8B**).

It is well accepted that during the (dark) catalytic reduction over bimetallic catalysts, using hydrogen as reducing agent, NO<sub>3</sub><sup>-</sup> is converted into NO<sub>2</sub><sup>-</sup> according to a redox reaction on the promoter metal (Cu). The role of the noble metal is to activate hydrogen, reducing the promoter metal, completing the catalytic cycle (Epron et al., 2001; Soares et al., 2011b; Zhang et al., 2013), being also active for the NO<sub>2</sub><sup>-</sup> reduction.

In the case of the photocatalytic process using metal-loaded TiO<sub>2</sub>, the mechanism generally proposed is based on the role of metal nanoparticles as electron sinks. Since the Fermi levels of noble metals are lower than that of TiO<sub>2</sub>, the photo-excited electrons can be transferred from the conduction band of the semiconductor to the metal nanoparticles deposited on its surface, being then available for NO<sub>3</sub><sup>-</sup> reduction (Kominami



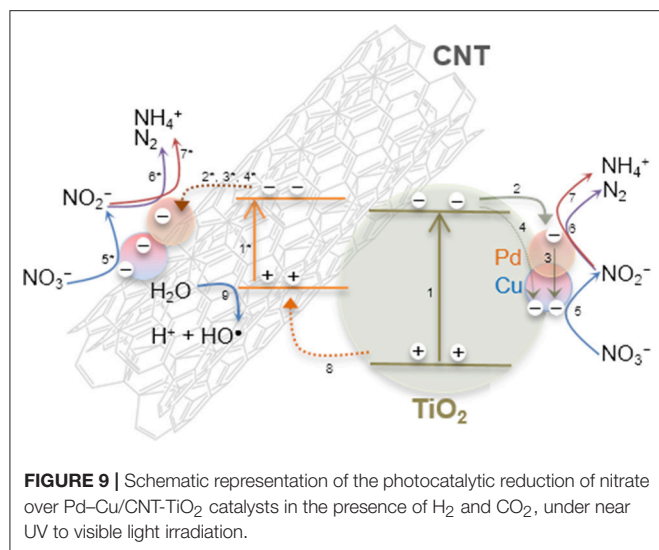
et al., 2005; Anderson, 2012; Soares et al., 2014). Hole scavengers are generally used, acting as sacrificial electron donors, avoiding electron-hole recombination. Yet, in the present work, no scavengers were added to the reaction medium.

The role played by CNT in CNT- $\text{TiO}_2$  hybrids has been discussed in previous works reporting the use of this type of materials as photocatalysts for environmental applications (Silva and Faria, 2010; Silva et al., 2015; Zeng et al., 2015; Yang and Park, 2017). CNT may act as adsorbent, as dispersing medium for  $\text{TiO}_2$  nanoparticles, it may span light absorption into the visible and may retard electron hole recombination. Although the surface area of the hybrid materials increased with CNT content, the first is not likely to be the most important effect, since no significant adsorption was observed whether the catalyst used.

TEM images of CNT- $\text{TiO}_2$  hybrids show that CNT promote the dispersion of  $\text{TiO}_2$  avoiding particle agglomeration (Figure 2). Moreover, the introduction of CNT increased the absorption of the resulting materials in the visible range, as shown by the UV-Vis spectra (Figure 5A), and lead to a decrease in the electron-hole recombination (Figure 5B).

Based in our findings, and considering the operation conditions used in this study, the following photocatalytic reaction mechanism is proposed. Since the irradiation source emits in the near UV to visible range, it is expected that  $\text{TiO}_2$  and CNT could be photoexcited simultaneously (Figure 9, steps 1 and 1\*).

After charge separation, electrons are transferred to Pd and Cu nanoparticles that are supported over  $\text{TiO}_2$  and also over



CNTs (Figure 9, steps 2–4), as observed by TEM (Figure 2). Photogenerated electrons may reduce both nitrate and nitrite adsorbed on Cu and Pd, respectively (Figure 9, steps 5–7). On the other hand, positively charged holes may migrate from TiO<sub>2</sub> to the CNT phase, where, in the absence of sacrificial electron donors, water can be oxidized to H<sup>+</sup> and HO<sup>•</sup> (Figure 9, steps 8 and 9). Hydroxyl radicals may indirectly re-oxidize byproducts to NO<sub>3</sub><sup>-</sup> (Tugaoen et al., 2017), while CO<sub>2</sub><sup>•-</sup>, which can be generated from the reduction of CO<sub>2</sub> (used as pH buffer) by available electrons, may play a role as reducing mediator (Zhang et al., 2005; Sá et al., 2009). The higher selectivity toward NH<sub>4</sub><sup>+</sup> production obtained using CNT-TiO<sub>2</sub> catalysts when irradiated may be rationalized by the excess of H<sup>+</sup> in the reaction medium, resulting from step 9 in Figure 9. Yet, no direct correlation between the CNT load in the hybrid materials and the selectivity toward NH<sub>4</sub><sup>+</sup> could be found (Figure 8B), which may derive from the complexity and simultaneity of the reactions involved in the mechanism of the photocatalytic process.

Although the photocatalytic process appears more advantageous in terms of kinetics of nitrate removal, the (dark) catalytic reactions using CNT-TiO<sub>2</sub> hybrid materials revealed to be more selective toward N<sub>2</sub> formation. Nevertheless, the possibility of using this type of materials may be envisioned as a cleaner route for the production of ammonia, comparing with the conventional fossil fuel based process (Yamauchi et al., 2011; Hirakawa et al., 2017).

## REFERENCES

- Anderson, J. A. (2011). Photocatalytic nitrate reduction over Au/TiO<sub>2</sub>. *Catal. Today* 175, 316–321. doi: 10.1016/j.cattod.2011.04.009
- Anderson, J. A. (2012). Simultaneous photocatalytic degradation of nitrate and oxalic acid over gold promoted titania. *Catal. Today* 181, 171–176. doi: 10.1016/j.cattod.2011.05.027
- Barrabés, N., Dafinov, A., Medina, F., and Sueiras, J. E. (2010). Catalytic reduction of nitrates using Pt/CeO<sub>2</sub> catalysts in a continuous

## CONCLUSION

TiO<sub>2</sub> and CNT-TiO<sub>2</sub> loaded with 1%Pd–1%Cu show high catalytic activity in the dark and under near UV to visible light irradiation, in the presence of H<sub>2</sub> and CO<sub>2</sub>. The presence of light promotes faster NO<sub>3</sub><sup>-</sup> conversion, due to the higher availability of reducing species. Carbon nanotubes induce to a positive effect in the selectivity of the catalytic reduction process toward N<sub>2</sub> formation. In the case of the photocatalytic process, the hybrid materials lead to an increase in the yield of the reduction of NO<sub>3</sub><sup>-</sup> to NH<sub>4</sub><sup>+</sup>, due to the high availability of H<sup>+</sup>. The efficiency of the hybrid materials depends on the CNT load, the best performing material being that composed by 20 wt.% of carbon nanotubes. In the case of the dark catalytic process, the synergic effect observed by the introduction of CNT in the TiO<sub>2</sub> matrix is mainly ascribed to the action of the carbon phase as dispersing medium to metal oxide particles, while under irradiation, CNT produce an increase in the efficiency of charge separation and mobility in the composite material.

## AUTHOR CONTRIBUTIONS

CS and OS conceived the research work, prepared and characterized the catalysts, performed the activity tests and drafted the manuscript. JÓ, MP, and JF provided the means for the realization of this work and contributed to the interpretation of the experimental results. All authors read and approved the final manuscript.

## FUNDING

This work was financially supported by Project POCI-01-0145-FEDER-006984—Associate Laboratory LSRE-LCM funded by FEDER through COMPETE2020—Programa Operacional Competitividade e Internacionalização (POCI)—and by national funds through FCT—Fundação para a Ciência e a Tecnologia, and by the project AIProcMat@N2020—Advanced Industrial Processes and Materials for a Sustainable Northern Region of Portugal 2020, with the reference NORTE-01-0145-FEDER-000006, supported by Norte Portugal Regional Operational Programme (NORTE 2020), under the Portugal 2020 Partnership Agreement, through the European Regional Development Fund (ERDF). CGS acknowledges the FCT Investigator Programme (IF/00514/2014) with financing from the European Social Fund and the Human Potential Operational Programme.

reactor. *Catal. Today* 149, 341–347. doi: 10.1016/j.cattod.2009.05.029

Calvo, L., Gilarranz, M. A., Casas, J. A., Mohedano, A. F., and Rodriguez, J. J. (2010). Denitrification of water with activated carbon-supported metallic catalysts. *Ind. Eng. Chem. Res.* 49, 5603–5609. doi: 10.1021/ie100838r

Dai, K., Zhang, X., Fan, K., Zeng, P., and Peng, T. (2014). Multiwalled carbon nanotube-TiO<sub>2</sub> nanocomposite for visible-light-induced photocatalytic hydrogen evolution. *J. Nanomater.* 2014:8. doi: 10.1155/2014/694073

- Devadas, A., Vasudevan, S., and Epron, F. (2011). Nitrate reduction in water: influence of the addition of a second metal on the performances of the Pd/CeO<sub>2</sub> catalyst. *J. Hazard. Mater.* 185, 1412–1417. doi: 10.1016/j.jhazmat.2010.10.063
- Doudrick, K., Yang, T., Hristovski, K., and Westerhoff, P. (2013). Photocatalytic nitrate reduction in water: managing the hole scavenger and reaction by-product selectivity. *Appl. Catal. B* 136–137, 40–47. doi: 10.1016/j.apcatb.2013.01.042
- Epron, F., Gauthard, F., Pineda, C., and Barbier, J. (2001). Catalytic reduction of nitrate and nitrite on Pt-Cu/Al<sub>2</sub>O<sub>3</sub> catalysts in aqueous solution: role of the interaction between copper and platinum in the reaction. *J. Catal.* 198, 309–318. doi: 10.1006/jcat.2000.3138
- Hirakawa, H., Hashimoto, M., Shiraiishi, Y., and Hirai, T. (2017). Photocatalytic conversion of nitrogen to ammonia with water on surface oxygen vacancies of titanium dioxide. *J. Am. Chem. Soc.* 139, 10929–10936. doi: 10.1021/jacs.7b06634
- Kapoor, A., and Viraraghavan, T. (1997). Nitrate removal from drinking water-review. *J. Environ. Eng.* 123, 371–380. doi: 10.1061/(ASCE)0733-9372(1997)123:4(371)
- Kominami, H., Nakaseko, T., Shimada, Y., Furusho, A., Inoue, H., Murakami, S., et al. (2005). Selective photocatalytic reduction of nitrate to nitrogen molecules in an aqueous suspension of metal-loaded titanium(IV) oxide particles. *Chem. Commun.* 23, 2933–2935. doi: 10.1039/b502909k
- López, R., Gómez, R., and Llanos, M. E. (2009). Photophysical and photocatalytic properties of nanosized copper-doped titania sol-gel catalysts. *Catal. Today* 148, 103–108. doi: 10.1016/j.cattod.2009.04.001
- Luiz, D. D. B., Andersen, S. L. F., Berger, C., José, H. J., and Moreira, R. D. F. P. M. (2012). Photocatalytic reduction of nitrate ions in water over metal-modified TiO<sub>2</sub>. *J. Photochem. Photobiol. A* 246, 36–44. doi: 10.1016/j.jphotochem.2012.07.011
- Marchesini, F. A., Gutierrez, L. B., Querini, C. A., and Miró, E. E. (2010). Pt,In and Pd,In catalysts for the hydrogenation of nitrates and nitrites in water. FTIR characterization and reaction studies. *Chem. Eng. J.* 159, 203–211. doi: 10.1016/j.cej.2010.02.056
- Martínez, J., Ortiz, A., and Ortiz, I. (2017). State-of-the-art and perspectives of the catalytic and electrocatalytic reduction of aqueous nitrates. *Appl. Catal. B* 207, 42–59. doi: 10.1016/j.apcatb.2017.02.016
- Prusse, U., Hahnlein, M., Daum, J., and Vorlop, K. D. (2000). Improving the catalytic nitrate reduction. *Catal. Today* 55, 79–90. doi: 10.1016/S.0920-5861(99)00228-X
- Sá, J., Agüera, C. A., Gross, S., and Anderson, J. A. (2009). Photocatalytic nitrate reduction over metal modified TiO<sub>2</sub>. *Appl. Catal. B* 85, 192–200. doi: 10.1016/j.apcatb.2008.07.014
- Sá, J., Berger, T., Föttinger, K., Riss, A., Anderson, J. A., and Vinek, H. (2005). Can TiO<sub>2</sub> promote the reduction of nitrates in water? *J. Catal.* 234, 282–291. doi: 10.1016/j.jcat.2005.06.015
- Sakamoto, Y., Kamiya, Y., and Okuhara, T. (2006). Selective hydrogenation of nitrate to nitrite in water over Cu-Pd bimetallic clusters supported on active carbon. *J. Mol. Catal. A Chem.* 250, 80–86. doi: 10.1016/j.molcata.2006.01.041
- Shand, M., and Anderson, J. A. (2013). Aqueous phase photocatalytic nitrate destruction using titania based materials: routes to enhanced performance and prospects for visible light activation. *Catal. Sci. Technol.* 3, 879–899. doi: 10.1039/c3cy20851f
- Silva, C. G., and Faria, J. L. (2010). Photocatalytic oxidation of benzene derivatives in aqueous suspensions: synergic effect induced by the introduction of carbon nanotubes in a TiO<sub>2</sub> matrix. *Appl. Catal. B* 101, 81–89. doi: 10.1016/j.apcatb.2010.09.010
- Silva, C. G., Sampaio, M. J., Marques, R. R. N., Ferreira, L. A., Tavares, P. B., Silva, A. M. T., et al. (2015). Photocatalytic production of hydrogen from methanol and saccharides using carbon nanotube-TiO<sub>2</sub> catalysts. *Appl. Catal. B* 178, 82–90. doi: 10.1016/j.apcatb.2014.10.032
- Soares, O. S. G. P., Órfão, J. J. M., and Pereira, M.F.R. (2009). Bimetallic catalysts supported on activated carbon for the nitrate reduction in water: optimization of catalysts composition. *Appl. Catal. B* 91, 441–448. doi: 10.1016/j.apcatb.2009.06.013
- Soares, O. S. G. P., Órfão, J. J. M., and Pereira, M.F.R. (2011a). Nitrate reduction in water catalysed by Pd-Cu on different supports. *Desalination* 279, 367–374. doi: 10.1016/j.desal.2011.06.037
- Soares, O. S. G. P., Órfão, J. J. M., and Pereira, M.F.R. (2011b). Nitrate reduction with hydrogen in the presence of physical mixtures with mono and bimetallic catalysts and ions in solution. *Appl. Catal. B* 102, 424–432. doi: 10.1016/j.apcatb.2010.12.017
- Soares, O. S. G. P., Órfão, J. J. M., Ruiz-Martínez, J., Silvestre-Albero, J., Sepúlveda-Escribano, A., and Pereira, M.F.R. (2010). Pd-Cu/AC and Pt-Cu/AC catalysts for nitrate reduction with hydrogen: influence of calcination and reduction temperatures. *Chem. Eng. J.* 165, 78–88. doi: 10.1016/j.cej.2010.08.065
- Soares, O. S. G. P., Pereira, M. F. R., Órfão, J. J. M., Faria, J. L., and Silva, C.G. (2014). Photocatalytic nitrate reduction over Pd-Cu/TiO<sub>2</sub>. *Chem. Eng. J.* 251, 123–130. doi: 10.1016/j.cej.2014.04.030
- Tahir, M., Tahir, B., and Amin, N. A. S. (2017). Synergistic effect in plasmonic Au/Ag alloy NPs co-coated TiO<sub>2</sub> NWs toward visible-light enhanced CO<sub>2</sub> photoreduction to fuels. *Appl. Catal. B* 204, 548–560. doi: 10.1016/j.apcatb.2016.11.062
- Tugaon, H. O., Garcia-Segura, S., Hristovski, K., and Westerhoff, P. (2017). Challenges in photocatalytic reduction of nitrate as a water treatment technology. *Sci. Total Environ.* 599–600, 1524–1551. doi: 10.1016/j.scitotenv.2017.04.238
- Wada, K., Hirata, T., Hosokawa, S., Iwamoto, S., and Inoue, M. (2012). Effect of supports on Pd-Cu bimetallic catalysts for nitrate and nitrite reduction in water. *Catal. Today* 185, 81–87. doi: 10.1016/j.cattod.2011.07.021
- Wu, Z., Sheng, Z., Wang, H., and Liu, Y. (2009). Relationship between Pd oxidation states on TiO<sub>2</sub> and the photocatalytic oxidation behaviors of nitric oxide. *Chemosphere* 77, 264–268. doi: 10.1016/j.chemosphere.2009.07.060
- Yamauchi, M., Abe, R., Tsukuda, T., Kato, K., and Takata, M. (2011). Highly selective ammonia synthesis from nitrate with photocatalytically generated hydrogen on CuPd/TiO<sub>2</sub>. *J. Am. Chem. Soc.* 133, 1150–1152. doi: 10.1021/ja106285p
- Yang, H. M., and Park, S. J. (2017). Effect of incorporation of multiwalled carbon nanotubes on photodegradation efficiency of mesoporous anatase TiO<sub>2</sub> spheres. *Mater. Chem. Phys.* 186, 261–270. doi: 10.1016/j.matchemphys.2016.10.052
- Zeng, Q., Li, H., Duan, H., Guo, Y., Liu, X., Zhang, Y., et al. (2015). A green method to prepare TiO<sub>2</sub>/MWCNT nanocomposites with high photocatalytic activity and insights into the effect of heat treatment on photocatalytic activity. *RSC Adv.* 5, 13430–13436. doi: 10.1039/C4RA13809K
- Zhang, F., Jin, R., Chen, J., Shao, C., Gao, W., Li, L., et al. (2005). High photocatalytic activity and selectivity for nitrogen in nitrate reduction on Ag/TiO<sub>2</sub> catalyst with fine silver clusters. *J. Catal.* 232, 424–431. doi: 10.1016/j.jcat.2005.04.014
- Zhang, R., Shuai, D., Guy, K. A., Shapley, J. R., Strathmann, T. J., and Werth, C. J. (2013). Elucidation of nitrate reduction mechanisms on a Pd-In bimetallic catalyst using isotope labeled nitrogen species. *ChemCatChem* 5, 313–321. doi: 10.1002/cctc.201200457
- Zhang, Y., Zhang, N., Tang, Z. R., and Xu, Y. J. (2012). Improving the photocatalytic performance of graphene-TiO<sub>2</sub> nanocomposites via a combined strategy of decreasing defects of graphene and increasing interfacial contact. *Phys. Chem. Chem. Phys.* 14, 9167–9175. doi: 10.1039/c2cp41318c

**Conflict of Interest Statement:** The authors declare that the research was conducted in the absence of any commercial or financial relationships that could be construed as a potential conflict of interest.

Copyright © 2018 Silva, Pereira, Órfão, Faria and Soares. This is an open-access article distributed under the terms of the Creative Commons Attribution License (CC BY). The use, distribution or reproduction in other forums is permitted, provided the original author(s) and the copyright owner(s) are credited and that the original publication in this journal is cited, in accordance with accepted academic practice. No use, distribution or reproduction is permitted which does not comply with these terms.